

See discussions, stats, and author profiles for this publication at: <https://www.researchgate.net/publication/268194921>

Mosaicking thermal images of buildings

Conference Paper in Proceedings of SPIE - The International Society for Optical Engineering · May 2013

DOI: 10.1117/12.2019985

CITATION

1

READS

147

5 authors, including:



Luigi Barazzetti

Politecnico di Milano

123 PUBLICATIONS 1,257 CITATIONS

SEE PROFILE



Silvia Erba

Politecnico di Milano

7 PUBLICATIONS 7 CITATIONS

SEE PROFILE



Elisabetta Rosina

Politecnico di Milano

65 PUBLICATIONS 314 CITATIONS

SEE PROFILE



Marco Scaioni

Politecnico di Milano

176 PUBLICATIONS 2,057 CITATIONS

SEE PROFILE

Some of the authors of this publication are also working on these related projects:



microclimate of historic buildings [View project](#)



thermography and cultural heritage, building inspection and moisture detection [View project](#)

Mosaicking thermal images of buildings

Luigi Barazzetti ^a, Silvia Erba ^a, Mattia Previtali ^a, Elisabetta Rosina ^a, Marco Scaioni ^b

^a Politecnico di Milano, Department of Building Environmental Science and Technology
Piazza Leonardo da Vinci 32, Milan, Italy
(elisabetta.rosina, luigi.barazzetti)@polimi.it, (silvia.erba, mattia.previtali)@mail.polimi.it,

^b Tongji University, Centre for Spatial Data Analysis and Sustainable Development Applications
College of Surveying and Geo-Informatics
1239 Siping Road, 200092 Shanghai, P.R. China
marco@tongji.edu.cn

ABSTRACT

Nowadays several thermal cameras capture images based on a pinhole camera model. This paper shows how multiple images of flat-like objects or fully 3D bodies can be mapped and mosaicked with a mathematical formulation between image and object spaces. This work demonstrates that both geometric and radiometric parts need proper mathematical models that allow the user to obtain a global product where the effective stored value in the measured temperature.

Keywords: Infrared thermography, GIS, photogrammetry, sensor fusion, texture mapping

1. INTRODUCTION

Image-based 3D reconstruction is the process where a real object photographed from different points of view is modeled by using a mathematical formulation between the images and object space. Several scientific work, along with many practical applications, illustrate different approaches and techniques, with variable levels of automation and requisites of the produced result in terms of accuracy, completeness, level of detail, metric scale, etc.

Most applications are nowadays carried out with pinhole cameras that produce central perspectives often degraded by a distortion due to the lens [1]. On the other hand, the use of such camera model is not the unique solution since alternative approaches based on push-broom, cylindrical, spherical, or other camera models were developed. The rapid diffusion of software implementation mainly based on pinhole cameras is essentially due to the availability of these sensors, where the market is continuously growing. A calibrated digital camera [2] can be intended as a rapid measuring tool with a limited cost: anyone has a digital camera today as it is one of the easiest tool to record and remember our special memories. In addition, multiple images coupled with 3D modeling algorithms allow operators not very expert in the field of 3D modeling to obtain good visual model without manual measurements (say user's interaction). Examples are free or low-cost packages such as 123DCatch and Photoscan. Some papers (e.g. [3-4]) proved how automated and accurate reconstructions are today feasible.

In this paper the work is extended from RGB images towards thermal ones where there is a lack of software able to deal with the temperature information, especially in the case of multiple images of complex 3D objects. Thermal infrared cameras operate in the bandwidth $3.5 \mu\text{m} < \lambda < 14 \mu\text{m}$ (Long Wave IR) and allows one to visualize thermal differences on the surface of an object. As is well known from Wien's displacement law, the maximum emitted electro-magnetic wavelength (λ_{max}) of an object is inversely proportional to its absolute temperature (T): $\lambda_{\text{max}}=2897.8/T$. This means that the higher the temperature, the shorter the maximum wavelength emitted. For instance, in the field of building analysis, the detection of temperatures in the range between -20 and 100 °C is required, corresponding to emitted maximum wavelengths ranging from $7.7 \mu\text{m}$ to $11.4 \mu\text{m}$. As a result, the sensors to be adopted must be able to work in the Long Wave IR spectrum.

A second problem concerning the sensor technology is related to the minimum size of the sensor unit, depending upon the diameter (d) of the diffraction disk: $d=2.44 \lambda k$, where λ is the wavelength of the recorded signal and $k = f/D$ (called “F” or “stop” number) is the ratio between focal length (f) and lens aperture (diameter of the pupil) (D). According to the shorter value of λ implied in the IR spectrum with respect to the visible one, resulting diffraction diameters will be much larger. As a consequence, while SLR (Single-Lens Reflex) cameras can be equipped with CCD (Charge-Coupled Device) or CMOS (Complementary Metal Oxide Semiconductor) sensors having a pixel size of a few micrometers, thermal cameras range between 30 and 50 μm .

Currently, cameras with sensor size inferior to 320×240 pixels can be purchased for a few thousand euros. Larger sensors are also available (up to a size of $1,280 \times 960$ pixels), although at an absolutely different cost. The most largely adopted technology is based on thermal detectors, which feature a sensitivity in the order of ± 0.1 K.

Thermocameras are based on a solid state sensor technology and can be handled as standard RGB cameras in photogrammetric applications. The pinhole camera model is here used, with lens distortion calibrated by standard photogrammetric procedures. This allows one to determine the internal geometry of the sensor and write a set of equations describing the relationship between images and object without including errors due to image distortion. This step is described in the next section, along with the procedure to manage multiple thermal images, mosaic them onto a complex 3D model of an object and preserve the measured temperature value.

2. GEOMETRIC MODEL

2.1 Overview

As mentioned, most IR cameras are capable of capturing small rectangular images based on a pinhole camera model. In the case of big objects or when the temperature information has to be related to the three-dimensional structure of a building, the independent analysis of single images could be insufficient. Images have to be mapped and mosaicked on the surfaces to be analyzed, often reconstructed with a 3D model [5].

In the case of small and flat surfaces, mapping an image is reduced to the computation of a homography. This requires the identification of at least four corresponding points on both IR image and surface, operation that could be difficult in many practical applications. The following sections show how thermal images can be processed in order to deal with fully 3D objects.

2.2 Thermal camera calibration

Thermal images based on the pinhole camera model often have geometric errors due to image distortion. This means that the measured image coordinates have to be corrected by using a proper mathematical model to take into consideration different errors. Image distortion is universally represented with an 8-term mathematical model. This is made up of 3 interior orientation parameters, 3 coefficients of radial distortion (k_1, k_2, k_3), and 2 coefficients of decentring distortion (p_1, p_2).

Interior orientation parameters are elements needed to describe the internal geometry of an image without distortion. They are made up of the distance c between the projection center, and the image plane projection of the perspective center onto the image plane that often has a residual offset (x_0, y_0). Radial distortion is instead modeled with an odd-ordered polynom series:

$$\delta r = k_1 r^3 + k_2 r^5 + k_3 r^7 \quad (1)$$

where r is the radial distance from the principal point. A misalignment of lens elements along the optical axis instead generates decentring distortion. The corrections of the image coordinates are given by:

$$\begin{aligned} \Delta x &= p_1 \left[r^2 + 2(x - x_0)^2 \right] + 2p_2 (x - x_0)(y - y_0) \\ \Delta y &= p_2 \left[r^2 + 2(y - y_0)^2 \right] + 2p_1 (x - x_0)(y - y_0) \end{aligned} \quad (2)$$

A standard photogrammetric procedure for camera calibration was used to obtain the 8 unknown parameters of different thermal cameras. This is based on a calibration framework made up of 38 control points (CPs) fixed on a wooden structure (Fig. 1). A set of iron nails were as CPs, whose 3D coordinates have been accurately measured by using a

theodolite from multiple stations. The precision of CPs is then much higher than the geometric resolution of the IR images. All the unknowns can be computed through a bundle adjustment. In the application carried out up until today, the measurement of the image coordinates of CPs is performed manually.

The mathematical model for image orientation [5] requires that the perspective centre, the image point, and the object point lie on a line in space. This transformation from image space (x, y) to object space (X, Y, Z) can be written as a 7-parameter transformation:

$$\begin{bmatrix} x - x_0 + \delta x + \Delta x \\ y - y_0 + \delta y + \Delta y \\ -c \end{bmatrix} = \lambda \mathbf{R} \begin{bmatrix} X - X_0 \\ Y - Y_0 \\ Z - Z_0 \end{bmatrix} \quad (3)$$

where \mathbf{R} is a 3×3 rotation matrix that depends on 3 angles, λ a scale factor, and $X_0 = [X_0, Y_0, Z_0]^T$ contains the coordinates of the perspective centre of the image.

An example is shown in Fig. 1, where the polygon used and the results of an adjustment process are shown. Camera poses (position and attitude) are estimated along with 3D point coordinates and calibration parameters.

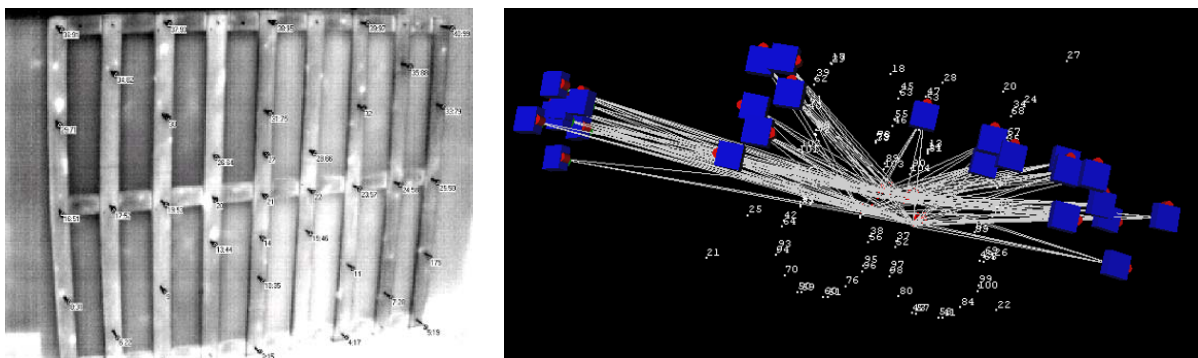


Figure 1. A thermal image of the calibration polygon and a 3D view of calibration project showing camera poses and 3D points.

2.3 Image orientation

Once the camera is calibrated, multiple images of the objects can be acquired to obtain a comprehensive visualization. The approach implemented not only use thermal images but standard RGB (say central perspectives) included in data processing. It is important to mention that the authors developed also an alternative procedure based on a special bi-stereo system [7-8]. This ‘bi-camera’ system includes an RGB and a thermal camera (Fig. 2), which allows the acquisition of particular image pairs. In this case the acquisition of thermal images was carried out by adopting a thermal long wave (8–13 μm) camera NEC H2640, with a geometric resolution of 640×480 pixels (other properties of the UFPA detector are: resolution 0.03°C , FoV $21.7^\circ \times 16.4^\circ$, IFOV 0.6 mrad). The RGB images were instead captured by a Nikon D80 camera (3872×2592 pixels) equipped with a 20 mm lens. The system is calibrated because the relative poses of both cameras can be computed: once position and attitude of the RGB camera is known, its corresponding thermal image can be oriented with a simple geometric transformation. It is easy to demonstrate that the needed parameters are a relative orientation matrix \mathbf{R}^* and a translation vector t , which are usually measured with a calibration project and then assumed as being constant for further analysis (if the system is stable).

In the case of a stereo system where cameras are mounted on a bar, the relative rotation matrix (\mathbf{R}^*) between both cameras can be expressed using the following condition:

$$\mathbf{R}^* = \mathbf{R}_{RGB}^T \mathbf{R}_{IR} \quad (4)$$

The matrix \mathbf{R}^* does not change if the stereo system is translated or rotated and can be determined with a calibration procedure where both thermal and visible images are oriented within a bundle adjustment using a photogrammetric block made up of stereo pairs. The knowledge of the rotation matrix \mathbf{R}_{RGB} is adopted to derive \mathbf{R}_{IR} by inverting Equation (3).

The second constraint due to relative orientation concerns the perspective centers of cameras. Although the length of the baseline $\|X_{0RGB} - X_{0IR}\|$ is a fixed value, the difference between the perspective center components ΔX cannot be a constant if the stereo system is shifted and rotated. On the other hand, if this difference is written by considering the reciprocal position of the cameras (e.g., using the intrinsic reference system of the right camera), it assumes a constant value t :

$$t = \mathbf{R}_{RGB}^T \Delta X \quad (4)$$

As a calibration project provides the value of the vector t , during the survey of a building façade the perspective center of the thermocamera can be estimated as:

$$X_{0IR} = \mathbf{R}_{RGB} t + X_{0RGB} \quad (5)$$

As the RGB camera is equipped with a short focal lens, a wide field of view is guaranteed. For this reason, data processing is carried out with RGB images only and then thermal images are oriented by knowing the relative position of both cameras. In other words, no measurement is carried out with thermal images. It is also noteworthy that (sometimes) RGB images can be automatically oriented with feature-based algorithms (like those presented in [13]) in order to speed up global processing.

This system was used for the north-eastern facades of ‘Trifoglio’ building at Politecnico di Milano (Fig. 7). The geometric model was created with a terrestrial laser scanning (TLS) Riegl LMS-Z420i equipped with a digital camera Nikon D100 (3008x2000 pixels). Two scans were acquired and registered by using a few retro-reflective targets. After registration, the whole point cloud was triangulated to obtain a polygonal model. This task can be accomplished in automatic way by using TLS processing software packages. The quality of the final model depends on the adopted resolution of the triangular mesh and on manual editing. Unfortunately, a time-consuming human intervention was needed to fill holes due to the lack of data, occlusions, and errors.

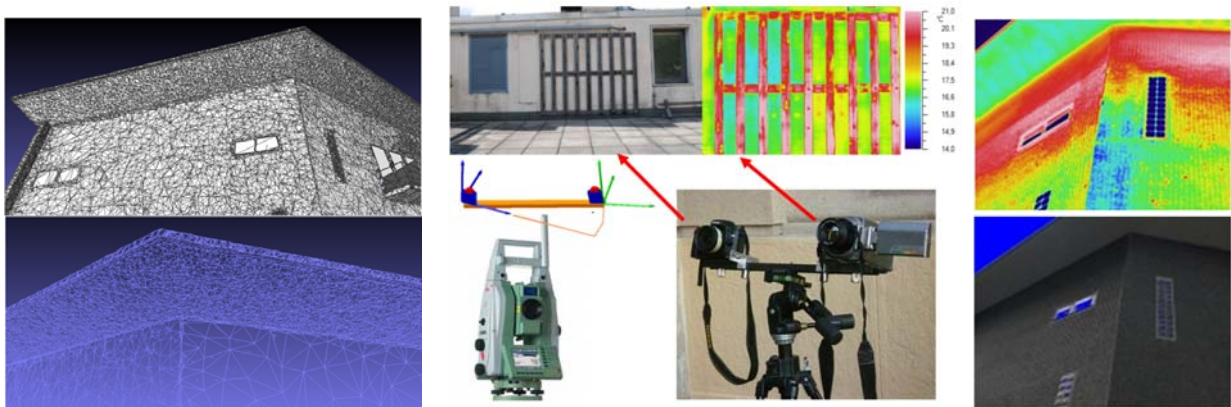


Figure 7. “Trifoglio” building, bi-camera system with integrated RGB and thermal cameras, and textured 3D model

An alternative method methodology here described uses both thermal and RGB images in a global photogrammetric bundle adjustment. The procedure starts with the acquisition of a preliminary set of RGB images with a calibrated camera, where it is necessary to consider the overlap between consecutive images. For instance, if the object is a simple planar facades, a strip of images with an overlap of 60% is a good solution, although terrestrial real cases suffer from other categories of problems and the expert photogrammetrist has to find a compromise.

RGB images are then oriented with standard photogrammetric methods from a set of image correspondences (tie points and ground control points to remove the rank deficiency: 7 parameters [9]). Tie points should guarantee not only a good distribution in the images in order to provide reliable orientation results, but also the possibility to orient all thermal images in a new adjustment project. This means that tie points should be measured in correspondence of elements that are visible in thermal data. In addition, as thermal images have a limited field of view, the manual measurement of many tie points is highly recommended, although this can lead to a longer processing time.

The method can be therefore intended as a first project with RGB images only. Then thermal data are added by measuring the image points already available in 3D. A final bundle adjustment including all data is finally carried out to obtain the exterior orientation parameters of all images.

There are some considerations to better understand the potential of this bundle formulation. First of all, the linearized model can be solved via Least Squares, and its solution is rigorous in a functional and stochastic sense. Then, thermal and RGB are employed together in order to obtain more precise and reliable results.

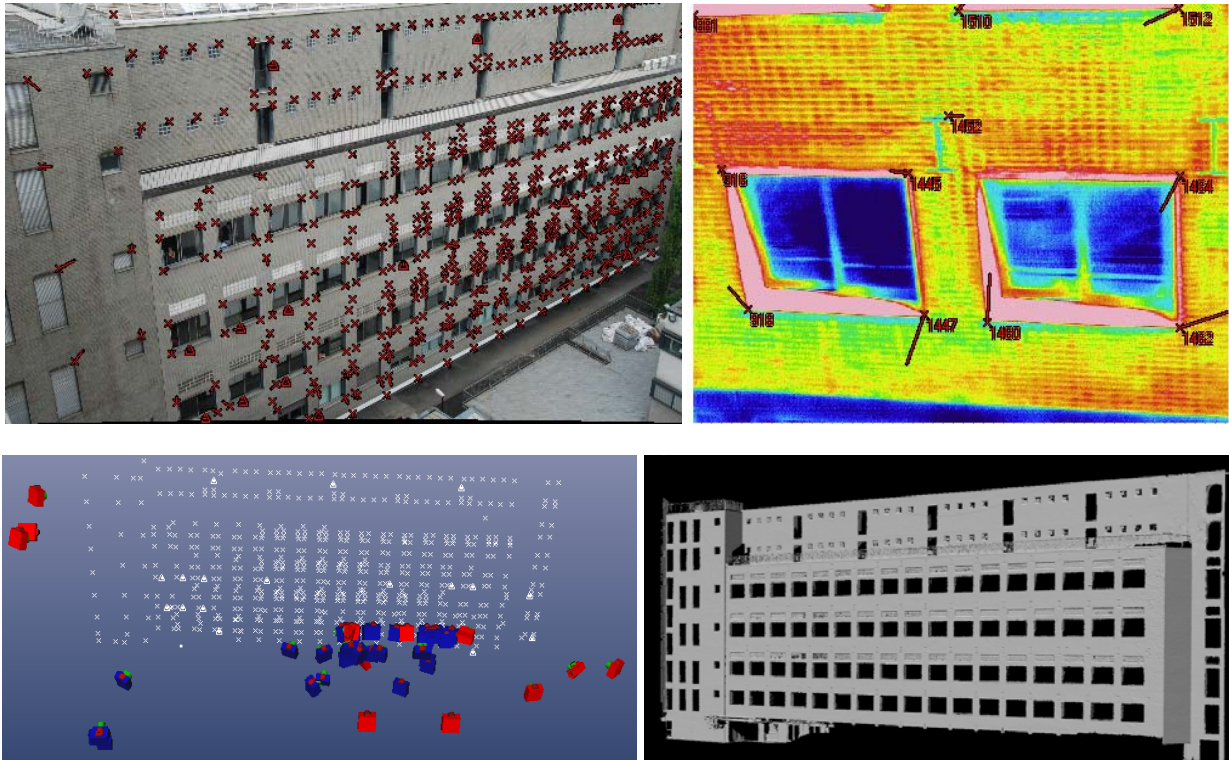


Figure 2. Combined adjustment of thermal and RGB images. As can be seen, points in the RGB image block are useful to orient all IR data with a combined bundle adjustment.

The main limit remains the manual measurement of many tie points, more than those strictly necessary for a standard photogrammetric project. In addition, the object must have a good texture where distinctive elements are visible in both thermal and RGB data.

3. RADIOMETRIC MODEL

RGB visual images of the temperature distribution are generally used for thermal analysis, thermography-textured 3D model generation and anomaly evaluation. These RGB images are obtained by transposing the temperature recorded by the IR sensor into a color space. Mapping from the temperature space to the RGB space is performed using some specific rules encoded in a designed. The transposition of temperatures to colors is a simple way to obtain a direct visualization of the temperature distribution of a surface. In addition, RGB images are very flexible: they can be visualized by image viewer software, processed in photogrammetric packages, incorporated in VRML models, etc. However, this kind of operation is not straightforward if the original temperature must be preserved.

RGB images can be essentially represented as 3D tensors. Each dimension of the tensor is an additive primary color component (or channel): Red, Green and Blue. In the RGB color space a generic color is described by indicating the components of the three additive primary colors by exploiting a specific range. From a computational point of view each

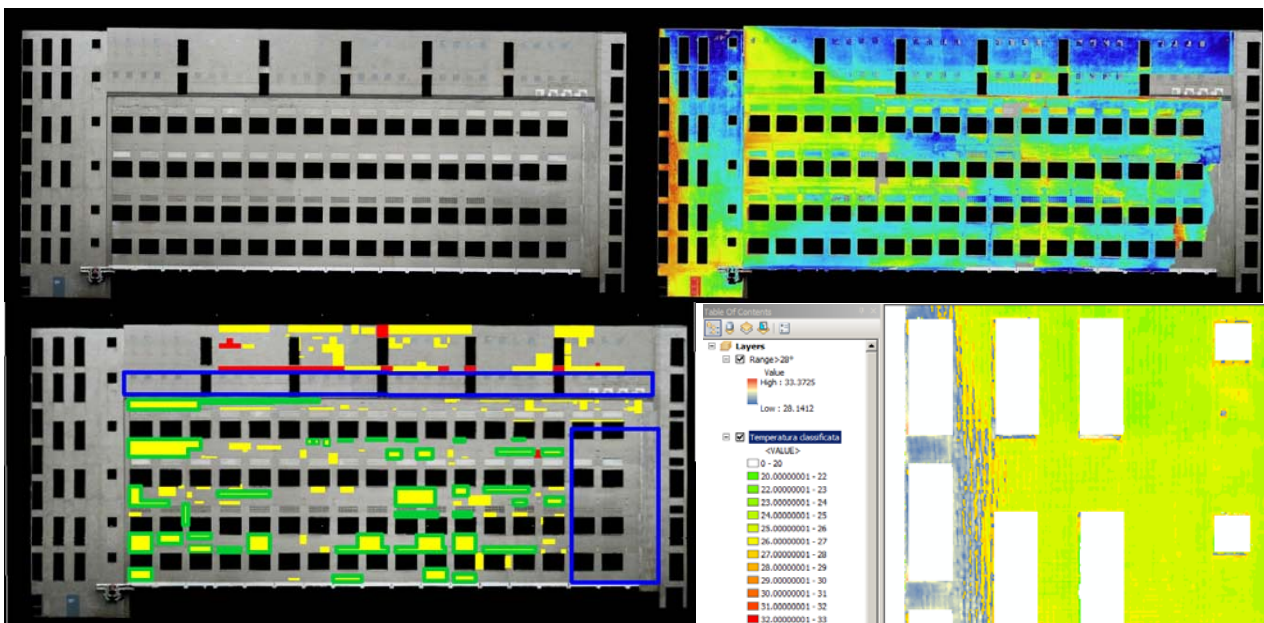
component of the tensor is an integer number varying from zero to a maximum value of $2n-1$, where n is the number of bits used to store the color information. Generally standard RGB sensors can record 8-bit, 12-bit or 16-bit per channel. IR sensors, instead, record temperature values in the range between -20 C and 100 C and have a sensitivity in the order of $\pm 0.1\text{ C}$. For this reason a thermal image can be represented as a matrix whose values are rational numbers with one digit.

As the two data structures are significantly different in many cases, software packages used for RGB images cannot be used for thermal images having temperature as pixel value. Although RGB visual images can overcome this problem, the original thermal information content is lost if the mapping role used between the two space is not known, and this is the case of many commercial software packages performing RGB mapping.

When the final product of an IRT survey is a thermographic orthophoto of a building façade, several thermal images have to be mapped and mosaicked on the surfaces to be analyzed. The process aimed at applying a surface texture to a 3D model is known as texture mapping. Images are selected by maximizing some score functions or optimizing some parameters such as the viewing direction, the level of detail, etc. Then, the texture is assigned to each triangle of the Triangulated Irregular Network (TIN) structure using the collinearity principle.

The algorithm here used is the one presented in [10], which is designed in order to minimize the effects of previously defined problems. This algorithm was developed for RGB texturing and its application to thermal images is not straightforward, as previously mentioned. In order to cope with this problem the temperatures recorded by IR cameras are encoded in a 16-bit gray value image. In other words, each temperature in the thermal image is mapped into a gray value between 0 and 65,535. This allows us to obtain a new RGB visual image but the advantage is given by the fact that the mapping between gray values and temperatures is known and can be inverted recovering temperature values in the following GIS analysis, as described in the next section.

The choice of 16-bit images is connected to the standard IRT applications. An 8-bit gray values image can encode only 256 gray tones which are less than 1200 possible temperature values obtainable working in the range between -20 C and 100 C at a sensitivity of $\pm 0.1\text{ C}$. A 16-bit gray value image encodes up to 65,536 gray tones, that is a sufficient margin in the case when wider range of temperatures or more sensible sensors are used. Once thermal images are converted into gray values they can be processed as standard RGB images obtaining the 3D textured model and deriving the 3D model, from which other products can be extracted. An example is shown in Fig. 3 (top) where the 3D model was textured by using a set of IR images. Fig. 3 (bottom) shows instead small details of a thermal orthophoto generated from multiple images is visualized in a GIS environment, where exhaustive analysis (e.g. the extraction of thermal gradients) can be easily performed combining radiometry and geometry.



4. CONCLUSION

This paper presented a mathematical approach able to deal with thermal images and derive rigorous image mosaics with temperature as radiometric value. Geometry and radiometry are taken into consideration in order to overcome some limitations of thermal cameras used in the field of IR object inspection.

Infrared thermography is today a quite popular tool for the inspection of buildings. On the other hand, sensors are used in a simplified way that limits the full potential of this technique. The method discussed and demonstrated along this paper increases the quality and relevance of achievable outputs. First of all, large and complex building facades can be textured in a rigorous way. Thanks to a detailed 3D model of the object that can be obtained on the basis of photogrammetry or laser scanning, the measured temperature value can be correctly assigned to each portion of the facade without rough approximations as in the case of simplified models.

Exportation of mapped temperatures in a desktop GIS then can help the users to apply spatial analysis that are typical of this kind of environment. Moreover, in the case of complex 3D objects current 2.5 GIS are not enough to deal with such data. Future development should concern the application of more involved 3D data structures able to handle full 3D geometries as well.

REFERENCES

- [1] Maldague, X., [Non Destructive Testing Handbook: Infrared and Thermal Testing], 3rd ed.; ASNT: Columbus, OH, USA, (2001).
- [2] Lagüela, S., González-Jorge, H., Armesto, J. and Arias, P., “Calibration and verification of thermographic cameras for geometric measurements”, *Infrared Phys. Technol.*, 54, 92-99, (2011).
- [3] Balaras, C. and Argiriou, A., “Infrared thermography for building diagnostics”, *Energy Build* 34(2):171-83, (2002).
- [4] Martín Ocaña, S., Cañas Guerrero, I. and González Requena, I., “Thermographic survey of two rural buildings in Spain”, *Energy Build* 36(6):515-23, (2004).
- [5] Ribarić, S., Marčetić, D. and Vedrina, D.S., “A knowledge-based system for the non-destructive diagnostics of façade isolation using the information fusion of visual and IR images”, *Expert Syst Appl* 36(2):3812-23, (2009).
- [6] Hartley, R.I. and Zisserman, A., [Multiple View Geometry in Computer Vision], Cambridge University Press, pp. 672 (2004).
- [7] Scaioni, M., Rosina, E., Barazzetti, L., Previtali, M. and Redaelli, V., “High-resolution texturing of building facades with thermal images”, *Proc. SPIE* 8354, 83540I (2012).
- [8] Alba, M.I., Barazzetti, L., Scaioni, M., Rosina, E. and Previtali M., “Mapping infrared data on terrestrial laser scanning 3D models of buildings”, *Remote Sensing* 3(9):1847-70, (2011).
- [9] Hoegner, L. and Stilla, U., “Thermal leakage detection on building façades using infrared textures generated by mobile mapping” In: *Proceedings of Joint Urban Remote Sensing Event (JURSE 2009)*. IEEE, Shanghai 6 p, (2009).
- [10] Pelagotti, A., Del Mastio, A., Ucheddu, F. and Remondino, F., “Automated multispectral texture mapping of 3D models”, *17th european signal processing conference*, Glasgow, (2009).
- [11] Rizzi, A., Voltolini, F., Girardi, S., Gonzo, L. and Remondino, F. “Digital preservation, documentation and analysis of paintings, monuments and large cultural heritage with infrared technology, digital cameras and range sensors”, *Proc. of XXI int. CIPA symposium*, (2007).
- [12] Rocchini, C., Cignoni, P., Montani, C., “Multiple Texture Stitching and Blending on 3D Objects” *Eurographics Rendering Workshop*, Granada, Spain (1999).
- [13] Bernardini, F., Martin, I.M. and Rushmeier, H., “High-quality texture reconstruction from multiple scans”, *Visualization and Computer Graphics*, *IEEE Transactions on* 7(4):318-32, (2001).
- [14] Callieri, M., Cignoni, P. and Scopigno, R., “Reconstructing textured meshes from multiple range rgb maps”, *7th int. l fall workshop on vision, modeling, and visualization 2002* pages 419–426, Erlangen (D), Nov. 20-22 2002, (2002).
- [15] Lempitsky, V. and Ivanov, D., “Seamless mosaicking of image-based texture maps”, *Computer vision and pattern recognition, 2007. CVPR '07. IEEE conference on*. 1 p, (2007).

- [16]Previtali, M., Scaioni, M., Barazzetti, L., Brumana, R. and Oreni, D., “An algorithm for occlusion-free texture mapping from oriented images”, ” In: Proceedings of “First International Conference on Software and Emerging Technologies for Education, Culture, Entertainment, and Commerce (SETECEC 2012), 10 pages, Venice (I), March 28 – 29, 2012, (2002).
- [17]ASTM C 1371 - 04, “Standard Test Method for Determination of Emittance of Materials Near Room Temperature Using Portable Emissometers”, 8 p, (2004).
- [18]ASTM E 1933 – 97, “Standard Test Methods for Measuring and Compensating for Emissivity Using Infrared Imaging Radiometers”, 962-3 p, (1997).